

Source Apportionment and Lung Cancer Risk Assessment of PM_{2.5}-Bound Polycyclic Aromatic Hydrocarbons in an Industrial City in Northwestern China

Feifei He

Shihezi University

Jianjiang Lu (✉ lujianjiang2021@163.com)

Shihezi University

Zilong Liu

Shihezi University

Junfeng Niu

Shihezi University

Zhuoying Li

Shihezi University

Research Article

Keywords: PAHs, PM_{2.5}, Health risk, PMF model, Backward trajectory, Shihezi city

Posted Date: February 4th, 2022

DOI: <https://doi.org/10.21203/rs.3.rs-1244748/v1>

License: © ⓘ This work is licensed under a Creative Commons Attribution 4.0 International License.

[Read Full License](#)

Abstract

In this study, we investigated the occurrence of particulate matter (PM_{2.5})-bound polycyclic aromatic hydrocarbons (PAHs) in the atmosphere in Shihezi, China and estimated their incremental lifetime cancer risk (ILCR). In addition, the potential sources of PM_{2.5}-bound PAHs were statistically estimated using principal component analysis and positive matrix factorization. The backward trajectory was employed to determine the potential source area using the HYSPLIT software. Concentrations of PM_{2.5} and 16 PM_{2.5}-bound PAHs ranged from 4.32 µg/m³ to 114.67 µg/m³ and 6.26 ng/m³ to 114.79 ng/m³, respectively, with the highest PAH concentrations occurring in the winter. Three principal components were analyzed by PCA, namely a combination of coal combustion sources and vehicle emissions, fugitive dust, and industrial emissions. Five sources were analyzed by positive matrix factorization (PMF) including coal combustion, vehicle emissions, fugitive dust, industrial emissions, and natural gas emissions. Risk assessment analysis showed that source-specific lung cancer risk assessment was in the 10⁻⁶–10⁻⁵ range, which constitutes a cancer risk that exceeds the guideline safety value (10⁻⁶) according to the U.S. Environmental Protection Agency. It is necessary to take measures to reduce the concentration of PM_{2.5}-bound PAHs in order to reduce human health hazards.

1. Introduction

The increase in numbers of motor vehicles(Li et al. 2019a), industrial units(Yadav et al. 2021), and rate of urbanization(Du et al. 2019) have led to the significant deterioration of ambient air quality (Kumar et al. 2011), especially in some developing regions of the world(Gan et al. 2021). Particulate matter (PM_{2.5}), with an aerodynamic diameter ≤ 2.5 µm(Vohra et al. 2021), is one of the main causes of air pollution. PM_{2.5} has a large specific surface area; thus, its surface adsorbs a variety of organic pollutants(Morawska et al. 2021), including polycyclic aromatic hydrocarbons (PAHs), which are widely scattered in the environment. In the atmospheric environment, PAHs are primarily derived from anthropogenic activities, including vehicle emissions (Luo et al. 2021), incomplete combustion of fossil fuels(Kim et al. 2013, Vohra et al. 2021), industrial emissions, and petroleum residue (Wang et al. 2022). The composition and toxicity of PAHs vary greatly depending on their sources. Some studies (Taghvaei et al. 2018, Wang et al. 2020a) used source-specific cancer risk assessment to verify that different sources pose different hazards to the human body. Therefore, it is necessary to fully understand the sources of PAHs and the toxicity caused by these different sources.

PAHs are significant organic pollutants in ambient air (Manisalidis et al. 2020, Yadav et al. 2020, Zhou et al. 2022), and mainly exist in the vapor and particle phases. They are common contaminants that can pollute areas not only near their sources, but also at receptor sites far away from their sources(Lin et al. 2020), as they can be transported long distances(Shrivastava et al. 2017). In addition, long-term and low-level exposure to PAHs may cause chronic health effects such as lung cancer, poor fertility outcomes, intestinal damage (Liu et al. 2021), and DNA damage(Wang et al. 2020b). Epidemiological studies have indicated that chronic exposure to PAHs is associated with decreased intelligence(Blazkova et al. 2020),

maternal demoralization(Rundle et al. 2012), asthma(Hu et al.), and obesity(Rundle et al. 2012). Stading et al indicated that PAHs in ambient air cause more lung cancer cases.

Shihezi, an important city in Xinjiang, is located along the Belt and Road. The topography of the Shihezi Reclamation Area from south to north consists of the Tianshan mountainous area, piedmont hilly area, piedmont slope plain, flood alluvial plain, and eolian desert area(Chen et al. 2019). Furthermore, special geographical environments and meteorological factors have caused the wind speed to decrease(Huang et al. 2021), which is not conducive to the diffusion of pollutants, especially particulate matter. In 2020, the air quality of Shihezi had 69.04% standard compliance, 11.23% light pollution, 5.47% moderate pollution, and 12.06% severe pollution, and 2.19% severe pollution, with the main pollutants being inhalable particulate matter.

The main objectives of this study were to (1) analyze the concentration level and distribution characteristics of 16 PM_{2.5}-bound PAHs in Shihezi from October 2020 through September 2021, (2) perform source-specific risk assessment of PM_{2.5}-bound PAHs by employing the PCA and the PMF models to distinguish the potential source profile of local emissions, and (3) evaluate the carcinogenic risk via inhalation exposure to PAHs for different groups of people.

2. Materials And Methods

2.1. Sampling location description and collection

Shihezi, an inland city located in the north of Xinjiang, is a rapidly developing city in northwestern China. Based on the distribution of urban functional areas, three sample points (S1, S2, and S3) were set up in three locations, as shown in Figure 1. The sampling locations were selected based on the comprehensive situation, including transport, convenience, and security. All sampling sites were 5 m above the ground, with no surrounding obstacles.

Particle sampling was carried out by employing low-volume air samplers with a flow rate of 16.7 L/min (manufactured by US BGI) to collect 23-h PM_{2.5}, using quartz filters (47 mm diameter, Whatman) from October 2020 through October 2021. Prior to sampling, the filters were pre-baked in a muffle furnace at 700°C for 5 h to remove organic compounds. The filter blanks were then processed in the same manner as the sample. All sampled filters were stored at -15°C until further analysis.

2.2. PAHs extraction and analysis

An accelerated solvent extraction (ASE) instrument was used to chemically extract 16 particle-bound PAHs. Half of the quartz filter was cut into small pieces and placed in the extraction tank. Extractions were performed under 100 bar, the hold time was 5 min, and the number of cycles was 2. After the sample was concentrated, we quantified and separated PM_{2.5}-bound PAHs using ultra performance liquid chromatography (UPLC). Detailed information from the 16 PAHs and instrument conditions are shown in Table S1 and Table S2.

2.3. Quality control and quality assurance

In this study, all operations and analysis processes strictly complied with quality assurance and quality control (QA/QC) procedures. First, we ensured the authenticity and accuracy of the samples during the sampling process. The flow rate of the particulate matter sampler was calibrated before and after sampling in each season and at each stage to ensure accurate flow. Second, we ensured quality control during the analysis process. Whole blanks, trip blanks, and laboratory blanks were analyzed using the same method used for sample analysis. Sixteen PAH standards were added to the blanks to calculate the recoveries, which were approximately 87.2–106.5%. The method detection limits (MDLs) were calculated as three times the standard deviation of the mean blank concentrations. In addition, the concentration of PAHs in the blank sample was below the detection limit of the method. The abbreviations of 16 PAHs were shown in Table S1. Regression equation, R^2 , detection limit and average recovery rate were shown in Table S2.

2.4. Source apportionment of PAHs

2.4.1. Principal Component Analysis (PCA)

Principal Component Analysis (PCA), a statistical method, was used to transform a group of potentially correlated variables into a group of linearly uncorrelated variables through orthogonal transformation (Ali-Taleshi et al. 2021a, Liu et al. 2017, Zhang et al. 2019), and this group of variables after conversion is called principal component. In this study, PCA was performed to determine the source of PAHs. The matrix can be analyzed by function 1:

$$X = YPT + E$$

1

where Y is the matrix of the principal component score, PT is a transposed matrix of principal component loadings, E is the matrix of residues, and X is the original PAH data matrix.

2.4.2. Positive Matrix Factorization Model

A positive matrix factorization (PMF) model with features such as uncertainties, estimation errors, unnecessary acquisition of information on sources, and emission inventory (a multivariate receptor tool) (Daellenbach et al. 2020), was employed to identify $PM_{2.5}$ bound PAH source profiles in Shihezi and quantify the contributions.

The concentration and uncertainty files are the two most important documents of the USEPA PMF. The former can be obtained from the monitoring results, and the latter can be obtained from the method detection limit (MDL) and error fraction. The uncertainty can be analyzed using the following function, if concentration >MDL:

$$uncertainty = \sqrt{(\text{Error} \times \text{concentration})^2 + (0.5 \times \text{MLD})^2}$$

2.1

else,

$$uncertainty = \frac{3}{4} \times MLD$$

2.2

2.4.3. Backward trajectory analysis

The 48-h backward trajectory clustering was computed using the HYSPLIT model at a height of 500 m above ground level, which is the most suitable height because the trajectory at this height has a significant effect on the PM_{2.5} concentration (Guan et al. 2019). The CWT model was used to identify the potential sources. It takes into account the residence time of the air mass in the grid (the longer the residence time, the greater the contribution of the trajectory to the sampling point). As shown in formula 3, the weight coefficients are used to reduce errors.

$$C_{ij} = \frac{1}{\sum_{l=1}^M \tau_{ijl}} \sum_{l=1}^M C_l \tau_{ijl}$$

3

2.5. Health risk assessment

At present, many studies and reports have mostly calculated the benzo(a)pyrene (BaP) equivalent concentration based on the toxicity equivalent factor to estimate PAH toxicity through respiratory exposure (Ali-Taleshi et al. 2021b, Liu et al. 2017). PAHs may interact with other toxic substances to increase their carcinogenicity. Therefore, the use of BaP alone might underestimate the toxic effects of PAHs (Ceratti et al. 2021). In this study, the carcinogenic equivalent concentration (BaP_{TEQ}) (Sanchez-Pinero et al. 2021) and the mutagenic equivalent concentration (BaP_{MEQ}) were chosen to estimate the carcinogenic and mutagenic concentrations of PM_{2.5}. The calculation formulas are as follows (4.1 and 4.2):

$$TEQ = \sum BEQ_i = \sum C_i \times TEF_i$$

4.1

$$MEQ = \sum BEQ_i = \sum C_i \times MEF_i$$

4.2

where C_i represents the concentration of the i-th PAH, TEF_i, and MEF_i, respectively, and indicate the toxic equivalency factor and mutagenic equivalent factor, respectively.

Lifetime carcinogenic risk based on the USEPA standard models was used to assess the carcinogenic risk of PAH exposure in humans. First, each exposure route was calculated, then the carcinogenic slope factor of each exposure route was multiplied to obtain the carcinogenic risk of each route, and finally the total carcinogenic risk was totaled (Wang et al. 2019). The calculation formula is as follows:

$$ILCR = Does_{Ingestion} \times SF_{Oral} + Does_{Inhalation} \times SF_{Inhalation} + Does_{Dermal} \times SF_{Dermal}$$

5

where $Does_{Ingestion}$, $Does_{Inhalation}$, and $Does_{Dermal}$ are the exposure doses (mg/kg/D) by ingestion, inhalation, and absorption, respectively. SF_{Oral} , $SF_{Inhalation}$, and SF_{Dermal} represent the carcinogenic slope factors of ingestion, inhalation, and absorption, respectively.

3. Result And Discussion

3.1. Spatial variation of PAHs concentrations

The spatial variation of Σ PAHs mass concentrations is shown in Table S1. The concentrations of Σ PAHs during the four seasons in point S1, point S2 and point S3 were in the ranges of 5.59–323.79 $\mu\text{g}/\text{m}^3$, 4.87–217.69 $\mu\text{g}/\text{m}^3$, and 7.44–312.55 $\mu\text{g}/\text{m}^3$, with annual mean concentrations (standard deviation, SD) of 58.04 $\mu\text{g}/\text{m}^3$, 37.12 $\mu\text{g}/\text{m}^3$, and 59.42 $\mu\text{g}/\text{m}^3$, respectively. The arterial road (point S1) and industrial district (point S3) displayed much higher mass concentrations of Σ PAHs than the living area (point S2), indicating that manufacturing facilities, power plants, and vehicle emissions cause more air pollution. Additionally, coal combustion, natural gas burning, and the burning of oil are the main sources of air pollution during the heating season in Shihezi.

3.2. Variation characteristics of PAHs in the heating and non-heating seasons

The four seasons of Shihezi are not obvious; spring and autumn are significantly shorter than summer and winter. In addition, the heating season lasts for about 6 months, from mid-October to mid-April of the following year. The average $\text{PM}_{2.5}$ -bound PAHs concentrations ranged from 16.50 ng/m^3 to 114.79 ng/m^3 (mean of 60.29 ng/m^3) and 6.26 ng/m^3 to 45.16 ng/m^3 (mean of 21.39 ng/m^3) in the heating season from the second half of 2020 to the first half of 2021 and non-heating season 2021, respectively. The changing trends of the total concentrations of PAHs and $\text{PM}_{2.5}$ in Shihezi are presented in Figure 2. The variation trend of the total concentration of PAHs was consistent with the $\text{PM}_{2.5}$, and the maximum concentrations of PAHs and $\text{PM}_{2.5}$ occurred in January, which was the coldest month during the sampling period. Additionally, the concentration of PAHs in the heating season was 2–3 times that of the non-heating season. Similar results have been reported in many other studies (Rajput & Lakhani 2009, Yan et al. 2019, Zhen et al. 2021), which showed that winter conditions typically lead to higher PAH concentrations. The seasonal pattern of PAHs was attributed to changes in the emission sources and meteorological conditions. Temperature is an important meteorological condition that affects the levels

of pollutants during the heating season. On one hand, temperature affects the migration and conversion of PAHs in the atmosphere(Dron et al. 2021); on the other hand, temperature greatly affects the heating demand, which indirectly affects the emission source. Hence, the lower the temperature, the higher the coal and natural gas emissions.

High molecular weight (HMW, 4–6 ring) PAHs are considered to be more toxic. However, the toxicity of low molecular weight (LMW, 2–3 ring) compounds cannot be ignored. In this study, both HMW and LMW PAHs were found in PM_{2.5}. As shown in Figure 3, the concentrations of 4-6 ring PAHs were 81.2% and 81.5% in the heating and non-heating seasons, respectively. 4-ring PAHs accounted for the highest proportion in the heating season, and 5-ring PAHs dominated during the non-heating season.

3.3. Correlation analysis

The Pearson correlation coefficient was calculated to study the possible relationship between PAHs and other pollutants and meteorological conditions. The scatterplot matrix of all pollutants and meteorological variables in the Pearson correlation are shown in Fig S1. The concentration of PM_{2.5}-bound PAHs had a strong positive correlation ($p < 0.001$) with the PM_{2.5}, indicating the higher the PM_{2.5} concentration, the higher the PAH concentration. PAH concentrations were positively correlated with the other pollutants (PM₁₀, SO₂, CO, NO₂, and O₃), except ozone. Moreover, temperature, wind speed, and visibility were significantly negatively correlated with PAH concentrations ($p < 0.001$), which could be due to the influence of these meteorological parameters on the chemical reaction, dispersion, and dilution process of particles bound to PAHs (Huang et al. 2021, Yin & Xu 2018). These results reflected the pronounced seasonal variations in PAH levels inversely following the ambient temperature, with higher concentrations during cold periods. First, PAH pollutants were more likely to condense in the atmosphere(Ren et al. 2021), and there will be more emissions under low temperature conditions. Next, as also occurred during the study performed by Masiol et al. (Masiol et al. 2013), higher wind speeds move large air masses and cause lower levels of particle-phase PAHs, whereas in the presence of scarce ventilation, locally emitted PAHs are trapped and concentrations increase.

3.4. PAHs source identification based on PCA and PMF

3.4.1. PCA analysis

PCA was performed to estimate the potential sources of PAHs in Shihezi. The results of the PCA are shown in Figure 4. Three principal components explained 64.3% of the total variance, with proportions of 44.2% for PC1, 12.4% for PC2, and 7.7% for PC3. Chrysene (Chr), benzo(b)fluoranthene (BbF), and benzo(k)fluoranthene (BkF) are indicators of coal combustion(Hamid et al. 2018), whereas acenaphthene (Ace), pyrene (Pyr), and BaP are mainly produced from vehicle emissions(Dhital et al. 2021, Smit et al. 2017). Thus, PC1 reflects a coal combustion and vehicle emissions source. PC2 was dominated by acenaphthylene (Acy), fluoranthene (Flu), and phenanthrene (Phe), which have a strong correlation with the source of fugitive dust(Cao et al. 2021, Han et al. 2009). Therefore, PC2 could explain fugitive dust.

PC3 was mainly defined by fluoranthene (Flu), BkF, and dibenzo(a,h)anthracene (DBA), which are interpreted as industrial emissions(Wu et al. 2021).

3.4.2. Source apportionment of PAHs by PMF

Figure S2 illustrates the correlations between the measured and model-predicted total PAH mass concentrations. Based on this, the PMF model was able to perfectly predict the total PAH mass concentrations, indicating that this model is suitable for PAH source apportionment.

Factor 1 was mainly defined by naphthalene (Nap), Pyr, and benzo(a)anthracene (BaA), which contributed 22.9% to the total PAH concentration, interpreted as natural gas emissions, as shown in Figure 5. Previous studies have shown that Pyr and BaA are typical tracers of natural gas(Li et al. 2019b). Xinjiang is rich in natural gas resources, which have been used as fuel for automobiles and households. Shihezi City has achieved full coverage of natural gas installations, which means that every household uses natural gas. In addition, the use of LNG in vehicles is trending because of low prices. Generally, the high-load low-ring aromatic hydrocarbons also verify that the combustion of LNG produces PAHs with lower and intermediate volatility (Mehmood et al. 2020).

Factor 2 explained 13.6% of the total PAH concentrations, and significant loadings of Ace, Fla, Pyr, Chr, BbF, DBA, and BaP are associated with this factor. According to previous studies, Pyr and Chr are chemical markers for industrial oil burning (Taghvaei et al. 2018). There are many factories in the north of Shihezi, most of which are chemical factories, such as factories producing acetylene, ethylene glycol, formaldehyde, and polyethylene, leading to an increase in gaseous and PM_{2.5} pollutants. DBA, BaP, and BkF have been previously observed as the dominant species in the ambient air of industrial sites (Rajput &Lakhani 2009).

Factor 3 accounted for 14.6% of the total PAH concentrations and it had a high loading of 3–4 ring PAHs, composed of Nap, Acy, Flu, Ace, Phe, anthracene (Ant), Pyr, and Chr. Phe, Pyr, and Chr are tracers for fugitive dust (Wang et al. 2020a), including coal, road floating soil, farmland soil, and construction waste. Shihezi has a temperate continental climate with sparse precipitation throughout the year and a dry climate, which causes the dust to enter the atmosphere for a long time, making it difficult to stabilize. In addition, the contribution of road dust and farmland soil to this source is not negligible as traffic flow has been increasing.

For factor 4, the main PAHs included BbF, BkF, BaP, DBA, indeno(1,2,3-cd)pyrene (Icdp), and benzo(ghi)perylene (Bghip), which are mainly generated from traffic emissions (Jia et al. 2018), accounting for 30.9%. Previous studies (Arellano et al. 2018, Mehmood et al. 2020, Rajput &Lakhani 2009, Sei et al. 2021) have shown that BbF, BkF, dibenzo(a,h)anthracene (DahA), and BghiP are specific tracers for traffic emissions, among which BbF, BaP, and BghiP are typical emission markers of gasoline vehicles. The contribution of automobile sources to PAHs is mainly due to the substantial increase in the number of automobiles in recent years, and there were obvious arterial roads near the sampling points. The lowest contribution to this source occurs in winter, but there is no seasonal change in traffic flow near

the sampling point. This may be due to the poor performance of the car engine exhaust control system at low temperatures (Pham et al. 2013, Zhou et al. 2005).

Factor 5 was primarily contributed by Nap, Acy, Flu, Ace, Phe, Ant, Fla, and Pyr, accounting for 17.9%, interpreted as a coal combustion source. Studies by Zou *et al.* (Zou et al. 2015) and Jamhari *et al.* (Jamhari et al. 2014) showed that these substances are direct markers of coal combustion. The contribution of coal-fired sources to PAHs is less than that of automobile sources and natural gas sources, due to the local government's achievements in coal substitution. However, the contribution of coal sources to PAHs in winter has significantly increased because coal is still the primary fuel source in this area, which is used in power plants and central heating system (Zhang et al. 2021). In addition, the contribution of coal sources in spring was also relatively high, which is related to the six-month heating season in Shihezi.

3.5. Backward trajectory analysis

Figure 6 shows the source direction and proportion of backward trajectory clustering of the four seasons during the sampling period. Shihezi, the largest province in China, is located in the north of Xinjiang. Therefore, most of the trajectories came from Xinjiang, and a small portion of the trajectories came from countries bordering Xinjiang. In winter, the air mass of cluster 1 came from the northeast of Xinjiang, accounting for 6.45%, which is a short-distance transportation. Both cluster 2 and cluster 4 were from the western part of Xinjiang. The former accounted for 22.85%, and the latter accounted for 10.89%. Cluster 3 was the air mass with the largest proportion (41.26%), which belongs to the local transportation around Shihezi. This indicates that winter heating caused this result. Additionally, the source contribution of around Urumqi cannot be ignored, and the air mass from this part is cluster 5 in the figure. Cluster 6 originated in Kazakhstan and reached Shihezi after long-distance transportation. In spring, clusters 1 and 3, accounting for 71.5% of the total air masses, came from short-distance transportation in the northeast and southwest directions of Shihezi, respectively. Clusters 2 and 6 both came from long-distance transportation in Kazakhstan, accounting for 11.69% and 4.44%, respectively. In summer, clusters 1, 3, and 5 were all from Kazakhstan, accounting for 23.19%, 14.03%, and 5.97%, respectively. Trajectory 2 comes from Karamay, an oil field city, which contributes to the high polycyclic aromatic hydrocarbons in Shihezi. Figure 6 clearly shows that the sources were roughly the same in summer and autumn. In autumn, cluster 1 had the highest proportion (27.55%), followed by cluster 3 (24.19%). Both originated from short-distance transportation. Clusters 4 and 6 were from the Ili Kazakh Autonomous Prefecture and Altay Region, respectively. The other two trajectories were from Kazakhstan.

The figure 7 shows the WPSCF analysis result of Shihezi's backward trajectory. A larger WPSCF value indicates that this area has a greater impact on the local PAHs. In winter, there were many concentrated areas where the CWT value was greater than 100, mainly in the surrounding areas of Shihezi. This may be due to temperature inversion in winter, which is not conducive to the diffusion of pollutants. In addition, the CWT value in autumn was roughly the same as the distribution in winter, and the potential source was located near Shihezi, which may have been caused by biomass burning in the surrounding area in autumn. In contrast, there were relatively few areas with a CWT value greater than 60 in summer,

and they were chiefly distributed in Kazakhstan, which is far from Shihezi. The number of severely affected areas in spring was significantly lower than that in winter and autumn.

3.6. Source-specific lung cancer risk assessment

The health risk assessment for children and adults was conducted using a Monte Carlo simulation, and the BaP_{eq} and ILCR results are illustrated in Figure 8. The mean BaP_{eq} concentrations in winter, spring, summer and autumn were 10.97, 6.85, 5.52, 3.98 ng/m^3 , respectively, with an annual mean concentration of 6.83 ng/m^3 . Table S3 presents a comparison of the equivalent toxic concentrations of PAHs in this study with those reported in previous studies. Our results indicated that the total BaP_{eq} was moderate (29 ng/m^3) in Shihezi compared to other cities in northwest China. Similarly, the reported BaP_{eq} levels in two other foreign cities, namely Coruña (Sanchez-Pinero et al. 2021) and Novo Hamburgo (Ceratti et al. 2021), were as low as $2.7 \pm 3.0 ng/m^3$ and $3.85 \times 10^{-2} ng/m^3$, respectively, both being lower than the BaP_{eq} level observed in Shihezi. As shown in Figure 8, the ILCR value of PAH exposures in the four seasons ranged from 2.61×10^{-6} to 9.91×10^{-6} for child and adult, with all values being higher than the threshold value (10^{-6}), suggesting a potential cancer risk. The total risk followed the order of winter > spring > autumn > summer for both children and adults, which was consistent with the seasonal distribution order of PAHs. The ILCR for adults was higher than that for children, which may be related to an unhealthy lifestyle, frequent exposure, and higher body weight of adults.

Figure 9 presents the lung cancer risk for each of the PAH emission sources, simulated by the PMF model. Results showed that the contributions of every source to ILCR in winter, except for the contribution of vehicles emissions to children, exceeded the prescribed threshold value (10^{-6}). Coal combustion and fugitive dust were the major sources of PAHs, with significantly higher cancer risks than the others. In summer, vehicle emissions account for the largest proportion of cancer risk, with ILCR values of 1.42×10^{-6} for children and 1.98×10^{-6} for adults, both higher than the threshold value. In summer and autumn, the contribution of most sources to ILCR was less than the threshold, whether for children or adults, suggesting a negligible cancer risk. However, the sum of their contributions to ILCR was greater than the threshold, indicating a potential cancer risk. The above results indicated that strengthening the comprehensive management of coal combustion source, vehicle emissions, fugitive dust, industrial emissions, and nature gas emissions is important for public health.

4. Conclusion

Few studies have been conducted on industrial cities with unique climate and geographical conditions in the arid and semi-arid regions of northwest China, especially Xinjiang. During the development process, these cities will inevitably cause damage to the environment, thereby threatening the health of local residents. Therefore, it is necessary to monitor the highly toxic pollutants and use a variety of methods to trace their potential sources. This study uses principal component analysis and the PMF model to identify $PM_{2.5}$ -bound PAH sources, which will be of help in policy formulation.

The main objectives of this research was to carry out the concentration distribution, analyze source apportionment based on multiple methods (PCA, PMF, and backward trajectory), and assess source-specific lung cancer risk of ambient PM_{2.5}-bound polycyclic aromatic hydrocarbons (PAHs) in Shihezi. The annual concentration of PAHs in the four seasons in Shihezi ranged from 4.87 µg/m³ to 323.79 µg/m³, and the concentration of PM_{2.5} ranged from 4.32 µg/m³ to 114.67 µg/m³. The variation trend of the total concentration of PAHs was consistent with the PM_{2.5} concentration. The PAH concentrations in the heating season was significantly greater than those during the non-heating season.

Through the PMF analysis, five main PAH emission sources in Shihezi city (PM_{2.5}) were apportioned, including coal combustion sources, vehicle emissions, fugitive dust, industrial emissions, and natural gas emissions, accounting for 17.9%, 30.9%, 14.6%, 13.6%, and 22.9% of the total PM_{2.5}-bound PAHs, respectively. The source-specific lung cancer risk assessment revealed that the calculated mean ILCR of PAHs for both children and adults was highest in winter, with values of 7.11×10^{-6} and 9.90×10^{-6} , respectively, outriding the threshold value (10^{-6}). The coal combustion source contributed the highest ILCR levels in winter (2.07×10^{-6}) and vehicle emissions accounted for the largest proportion of ILCR in spring (1.70×10^{-6}), indicating a potential cancer risk. In summer and autumn, the contribution of the five sources to the ILCR was less than the threshold, suggesting a negligible cancer risk. To reduce the risk of PM_{2.5}-bound PAH exposure to carcinogenesis, it is recommended to reduce the consumption of coal, diesel, and gasoline by using clean energy instead of fossil fuel technology to control air pollution. Avoiding outdoor activities and wearing a mask are effective ways to reduce the carcinogenicity of PAHs, especially in winter during severe pollution.

Declarations

Funding

This work was supported by the National Natural Science Foundation of China (grant number 21866029).

Competing Interests

The authors have no relevant financial or non-financial interests to disclose.

Author Contributions

Feifei He: Validation, conceptualization, investigation, visualization, writing–original draft, writing–review and editing. **Jianjiang Lu:** Validation, resources, conceptualization, supervision, writing - review and editing. **Zilong Liu:** Validation and supervision **Junfeng Niu:** Validation and supervision **Zhuoying Li:** Validation and investigation. All authors read and approved the final manuscript.

Date availability

The data and materials presented in this study are available on request from the corresponding author. The data are not publicly available due to privacy restrictions.

Ethics declarations

Ethics approval

Not applicable.

Consent to participate

Not applicable.

Consent for publication

All authors reviewed and approved the manuscript for publication.

Competing interests

The authors declare no competing interests.

References

1. Ali-Taleshi MS, Bakhtiari AR, Moeinaddini M, Squizzato S, Feiznia S, Cesari D (2021a) Single-site source apportionment modeling of PM_{2.5}-bound PAHs in the Tehran metropolitan area, Iran: Implications for source-specific multi-pathway cancer risk assessment. *Urban CLim* 39:18
2. Ali-Taleshi MS, Squizzato S, Bakhtiari AR, Moeinaddini M, Masiol M (2021b) Using a hybrid approach to apportion potential source locations contributing to excess cancer risk of PM_{2.5}-bound PAHs during heating and non-heating periods in a megacity in the Middle East. *Environ Res* 201:17
3. Arellano L, Fernandez P, van Drooge BL, Rose NL, Nickus U, Thies H, Stuchlik E, Camarero L, Catalan J, Grimalt JO (2018) Drivers of atmospheric deposition of polycyclic aromatic hydrocarbons at European high-altitude sites. *Atmos Chem Phys* 18:16081–16097
4. Blazkova B, Pastorkova A, Solansky I, Veleminsky M, Veleminsky M, Urbancova K, Vondraskova V, Hajslova J, Pulkrabova J, Sram RJ (2020) Effect of Polycyclic Aromatic Hydrocarbons Exposure on Cognitive Development in 5 Years Old Children. *Brain Sci* 10:11
5. Cao F, Zhang YX, Lin X, Zhang YL (2021) Characteristics and source apportionment of non-polar organic compounds in PM_{2.5} from the three megacities in Yangtze River Delta region, China. *Atmos Res* 252:12
6. Ceratti AM, da Costa GM, Alves DD, Cansi LM, Hansen J, Brochier F, de Quevedo DM, Osorio DMM (2021) Polycyclic Aromatic Hydrocarbons (PAH) in Atmospheric Particles (PM_{2.5} and PM_{2.5-10}): Integrated Evaluation of the Environmental Scenario in Urban Areas. *Water Air and Soil Pollution* 232:17

7. Chen JD, Lu JJ, Ning JY, Yan YJ, Li SM, Zhou L (2019) Pollution characteristics, sources, and risk assessment of heavy metals and perfluorinated compounds in PM_{2.5} in the major industrial city of northern Xinjiang, China. *Air Quality Atmosphere and Health* 12:909–918
8. Daellenbach KR et al (2020) Sources of particulate-matter air pollution and its oxidative potential in Europe. *Nature* 587:414–
9. Dhital NB, Wang SX, Lee CH, Su J, Tsai MY, Zhou YJ, Yang HH (2021) Effects of driving behavior on real-world emissions of particulate matter, gaseous pollutants and particle-bound PAHs for diesel trucks. *Environ Pollut* 286:11
10. Dron J, Ratier A, Austruy A, Revenko G, Chaspoul F, Wafo E (2021) Effects of meteorological conditions and topography on the bioaccumulation of PAHs and metal elements by native lichen (*Xanthoria parietina*). *J Environ Sci* 109:193–205
11. Du YY, Wan Q, Liu HM, Liu H, Kapsar K, Peng J (2019) How does urbanization influence PM_{2.5} concentrations? Perspective of spillover effect of multi-dimensional urbanization impact. *J Clean Prod* 220:974–983
12. Gan T, Yang HC, Liang W, Liao XC (2021) Do economic development and population agglomeration inevitably aggravate haze pollution in China? New evidence from spatial econometric analysis. *Environ Sci Pollut Res* 28:5063–5079
13. Guan QY, Yang YY, Luo HP, Zhao R, Pan NH, Lin JK, Yang LQ (2019) Transport pathways of PM₁₀ during the spring in northwest China and its characteristics of potential dust sources. *J Clean Prod* 237:12
14. Hamid N, Syed JH, Junaid M, Mahmood A, Li J, Zhang G, Malik RN (2018) Elucidating the urban levels, sources and health risks of polycyclic aromatic hydrocarbons (PAHs) in Pakistan: Implications for changing energy demand. *Sci Total Environ* 619:165–175
15. Han B, Bai ZP, Guo GH, Wang F, Li F, Liu QX, Ji YQ, Li X, Hu YD (2009) Characterization of PM₁₀ fraction of road dust for polycyclic aromatic hydrocarbons (PAHs) from Anshan, China. *J Hazard Mater* 170:934–940
16. Hu JY, Bao YL, Huang H, Zhang Z, Chen F, Li L, Wu Q The preliminary investigation of potential response biomarkers to PAHs exposure on childhood asthma. *J. Expo. Sci. Environ. Epidemiol.*,12
17. Huang YX, Guo B, Sun HX, Liu HJ, Chen SX (2021) Relative importance of meteorological variables on air quality and role of boundary layer height. *Atmos Environ* 267:10
18. Jamhari AA, Sahani M, Latif MT, Chan KM, Tan HS, Khan MF, Tahir NM (2014) Concentration and source identification of polycyclic aromatic hydrocarbons (PAHs) in PM₁₀ of urban, industrial and semi-urban areas in Malaysia. *Atmos Environ* 86:16–27
19. Jia JP, Bi CJ, Zhang JF, Jin XP, Chen ZL (2018) Characterization of polycyclic aromatic hydrocarbons (PAHs) in vegetables near industrial areas of Shanghai, China: Sources, exposure, and cancer risk. *Environ Pollut* 241:750–758
20. Kim KH, Jahan SA, Kabir E, Brown RJC (2013) A review of airborne polycyclic aromatic hydrocarbons (PAHs) and their human health effects. *Environ Int* 60:71–80

21. Kumar P, Gurjar BR, Nagpure AS, Harrison RM (2011) Preliminary Estimates of Nanoparticle Number Emissions from Road Vehicles in Megacity Delhi and Associated Health Impacts. *Environ Sci Technol* 45:5514–5521
22. Li K, Jacob DJ, Liao H, Zhu J, Shah V, Shen L, Bates KH, Zhang Q, Zhai SX (2019a) A two-pollutant strategy for improving ozone and particulate air quality in China. *Nat Geosci* 12:906–
23. Li Q, Jiang N, Yu X, Dong Z, Duan SG, Zhang LS, Zhang RQ (2019b) Sources and spatial distribution of PM_{2.5}-bound polycyclic aromatic hydrocarbons in Zhengzhou in 2016. *Atmos Res* 216:65–75
24. Lin Y, Liu L, Cai MG, Rodenburg LA, Chitsaz M, Liu YG, Chen M, Deng HX, Ke HW (2020) Isolating different natural and anthropogenic PAHs in the sediments from the northern Bering-Chukchi margin: Implications for transport processes in a warming Arctic. *Sci Total Environ* 736:9
25. Liu D, Lin T, Syed JH, Cheng ZN, Xu Y, Li KC, Zhang G, Li J (2017) : Concentration, source identification, and exposure risk assessment of PM_{2.5}-bound parent PAHs and nitro-PAHs in atmosphere from typical Chinese cities. *Sci Rep* 7
26. Liu JH, Su XH, Lu JJ, Ning JY, Lin M, Zhou HJ (2021) PM_{2.5} induces intestinal damage by affecting gut microbiota and metabolites of rats fed a high-carbohydrate diet. *Environ Pollut* 279:9
27. Luo KS, Zeng YQ, Li MH, Man YB, Zeng LX, Zhang QY, Luo JW, Kang Y (2021) Inhalation bioaccessibility and absorption of polycyclic aromatic hydrocarbons (PAHs) in indoor PM_{2.5} and its implication in risk assessment. *Sci Total Environ* 774:8
28. Manisalidis I, Stavropoulou E, Stavropoulos A, Bezirtzoglou E (2020) Environmental and Health Impacts of Air Pollution: A Review. *Front Public Health* 8:13
29. Masiol M, Formenton G, Pasqualetto A, Pavoni B (2013) Seasonal trends and spatial variations of PM₁₀-bounded polycyclic aromatic hydrocarbons in Veneto Region, Northeast Italy. *Atmos Environ* 79:811–821
30. Mehmood T, Zhu TL, Ahmad I, Li XH (2020) Ambient PM_{2.5} and PM₁₀ bound PAHs in Islamabad, Pakistan: Concentration, source and health risk assessment. *Chemosphere* 257:16
31. Morawska L et al (2021) The state of science on severe air pollution episodes: Quantitative and qualitative analysis. *Environ Int* 156:106732
32. Pham CT, Kameda T, Toriba A, Hayakawa K (2013) Polycyclic aromatic hydrocarbons and nitropolycyclic aromatic hydrocarbons in particulates emitted by motorcycles. *Environ Pollut* 183:175–183
33. Rajput N, Lakhani A (2009) Measurements of polycyclic aromatic hydrocarbons at an industrial site in India. *Environ Monit Assess* 150:273–284
34. Ren YQ, Wei J, Wu ZH, Ji YY, Bi F, Gao R, Wang XZ, Wang GH, Li H (2021) Chemical components and source identification of PM_{2.5} in non-heating season in Beijing: The influences of biomass burning and dust. *Atmos Res* 251:8
35. Rundle A, Hoepner L, Hassoun A, Oberfield S, Freyer G, Holmes D, Reyes M, Quinn J, Camann D, Perera F, Whyatt R (2012) Association of Childhood Obesity With Maternal Exposure to Ambient Air Polycyclic Aromatic Hydrocarbons During Pregnancy. *Am J Epidemiol* 175:1163–1172

36. Sanchez-Pinero J, Moreda-Pineiro J, Turnes-Carou I, Fernandez-Amado M, Muniategui-Lorenzo S, Lopez-Mahia P (2021) Polycyclic aromatic hydrocarbons in atmospheric particulate matter (PM₁₀) at a Southwestern Europe coastal city: status, sources and health risk assessment. *Air Quality Atmosphere and Health* 14:1325–1339
37. Sei KT, Wang Q, Tokumura M, Hossain A, Raknuzzaman M, Miyake Y, Amagai T (2021) : Occurrence, potential source, and cancer risk of PM_{2.5}-bound polycyclic aromatic hydrocarbons and their halogenated derivatives in Shizuoka, Japan, and Dhaka, Bangladesh. *Environ. Res.* 196
38. Shrivastava M, Lou S, Zelenyuk A, Easter RC, Corley RA, Thrall BD, Rasch PJ, Fast JD, Simonich SLM, Shen HZ, Tao S (2017) : Global long-range transport and lung cancer risk from polycyclic aromatic hydrocarbons shielded by coatings of organic aerosol. *Proc. Natl. Acad. Sci. U. S. A.* 114, 1246-1251
39. Smit R, Kingston P, Wainwright DH, Tooker R (2017) A tunnel study to validate motor vehicle emission prediction software in Australia. *Atmos Environ* 151:188–199
40. Taghvaei S, Sowlat MH, Hassanvand MS, Yunesian M, Naddafi K, Sioutas C (2018) Source-specific lung cancer risk assessment of ambient PM_{2.5}-bound polycyclic aromatic hydrocarbons (PAHs) in central Tehran. *Environ Int* 120:321–332
41. Vohra K, Vodonos A, Schwartz J, Marais EA, Sulprizio MP, Mickley LJ (2021) Global mortality from outdoor fine particle pollution generated by fossil fuel combustion: Results from GEOS-Chem. *Environ Res* 195:8
42. Wang LJ, Dong SZ, Liu MM, Tao WD, Xiao B, Zhang SW, Zhang PQ, Li XP (2019) Polycyclic aromatic hydrocarbons in atmospheric PM_{2.5} and PM₁₀ in the semi-arid city of Xi'an, Northwest China: Seasonal variations, sources, health risks, and relationships with meteorological factors. *Atmos Res* 229:60–73
43. Wang S, Qin JH, Xie BX, Sun H, Li X, Chen WQ (2022) Volatilization behavior of polycyclic aromatic hydrocarbons from the oil-based residues of shale drill cuttings. *Chemosphere* 288:10
44. Wang SB, Ji YQ, Zhao JB, Lin Y, Lin Z (2020a) Source apportionment and toxicity assessment of PM_{2.5}-bound PAHs in a typical iron-steel industry city in northeast China by PMF-ILCR. *Sci Total Environ* 713:12
45. Wang W, Ding X, Turap Y, Tursun Y, Abulizi A, Wang XM, Shao LY, Talifu D, An JQ, Zhang XX, Zhang YY, Liu HB (2020b) Distribution, sources, risks, and vitro DNA oxidative damage of PM_{2.5}-bound atmospheric polycyclic aromatic hydrocarbons in Urumqi, NW China. *Sci Total Environ* 739:13
46. Wu YJ, Xu ZY, Liu SQ, Tang MH, Lu SY (2021) Emission of organic components and distribution characteristics of PAHs in condensable particulate matter from coal-fired power and industrial plants. *J Energy Inst* 97:109–116
47. Yadav A, Behera SN, Nagar PK, Sharma M (2020) Spatio-seasonal Concentrations, Source Apportionment and Assessment of Associated Human Health Risks of PM_{2.5}-bound Polycyclic Aromatic Hydrocarbons in Delhi, India. *Aerosol Air Qual Res* 20:2805–2825
48. Yadav M, Singh NK, Sahu SP, Padhiyar H (2021) Investigations on air quality of a critically polluted industrial city using multivariate statistical methods: Way forward for future sustainability.

49. Yan DH, Wu SH, Zhou SL, Tong GJ, Li FF, Wang YM, Li BJ (2019) Characteristics, sources and health risk assessment of airborne particulate PAHs in Chinese cities: A review. *Environ Pollut* 248:804–814
50. Yin H, Xu LY (2018) Comparative study of PM10/PM2.5-bound PAHs in downtown Beijing, China: Concentrations, sources, and health risks. *J Clean Prod* 177:674–683
51. Zhang GZ, Ma KJ, Sun LJ, Liu PF, Yue YL (2021) Seasonal pollution characteristics, source apportionment and health risks of PM2.5-bound polycyclic aromatic hydrocarbons in an industrial city in northwestern China. *Hum Ecol Risk Assess* 27:1054–1071
52. Zhang J, Li RF, Zhang XY, Bai Y, Cao P, Hua P (2019) Vehicular contribution of PAHs in size dependent road dust: A source apportionment by PCA-MLR, PMF, and Unmix receptor models. *Sci Total Environ* 649:1314–1322
53. Zhen Z, Yin Y, Chen K, Zhen X, Zhang X, Jiang H, Wang H, Kuang X, Cui Y, Dai M, He C, Liu A, Zhou F (2021) : Concentration and atmospheric transport of PM2.5-bound polycyclic aromatic hydrocarbons at Mount Tai, China. *The Science of the total environment* 786,147513–147513
54. Zhou J-B, Wang T-G, Huang Y-B, Mao T, Zhong N-N, Zhang Y, Zhang X-S (2005) Concentration and distribution characterization of polycyclic aromatic hydrocarbons in airborne particles with different sizes. *Huan jing ke xue= Huanjing kexue* 26:40–44
55. Zhou Q, Chen J, Zhang J, Zhou F, Zhao J, Wei X, Zheng K, Wu J, Li B, Pan B (2022) : Toxicity and endocrine-disrupting potential of PM2.5: Association with particulate polycyclic aromatic hydrocarbons, phthalate esters, and heavy metals. *Environ. Pollut.* 292
56. Zou YH, Wang LX, Christensen ER (2015) Problems in the fingerprints based polycyclic aromatic hydrocarbons source apportionment analysis and a practical solution. *Environ Pollut* 205:394–402

Figures

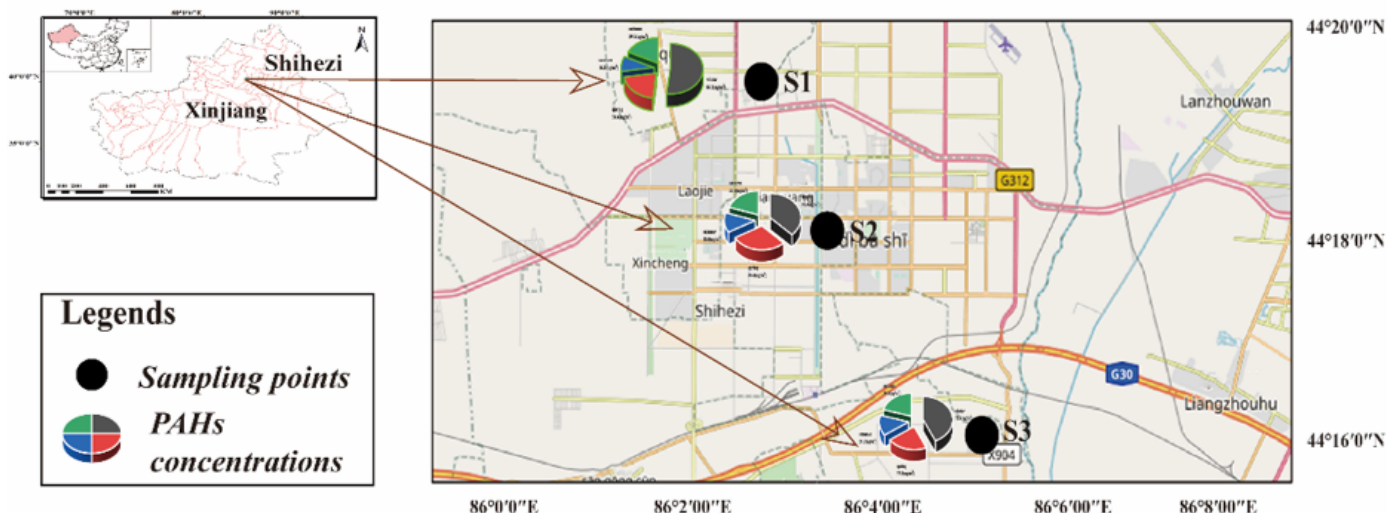


Figure 1

Sampling locations in Shihezi.

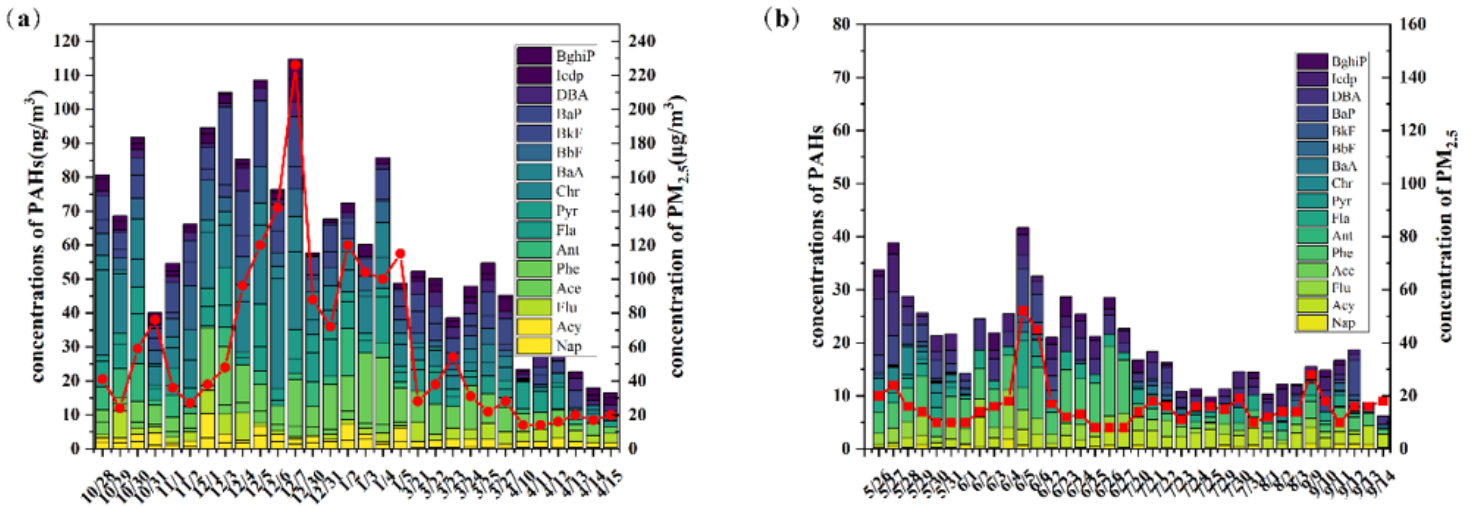


Figure 2

The concentration distribution of $PM_{2.5}$ and $PM_{2.5}$ -bound PAHs in the heating season (a) and non-heating season (b) in Shihezi

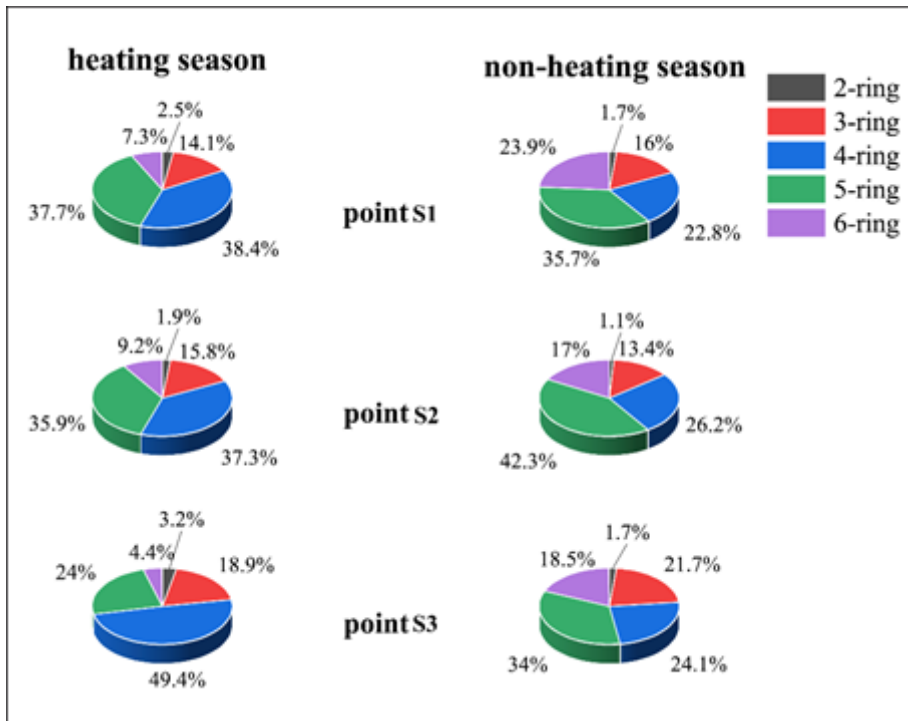


Figure 3

Percentage of 2-6 ring PAHs

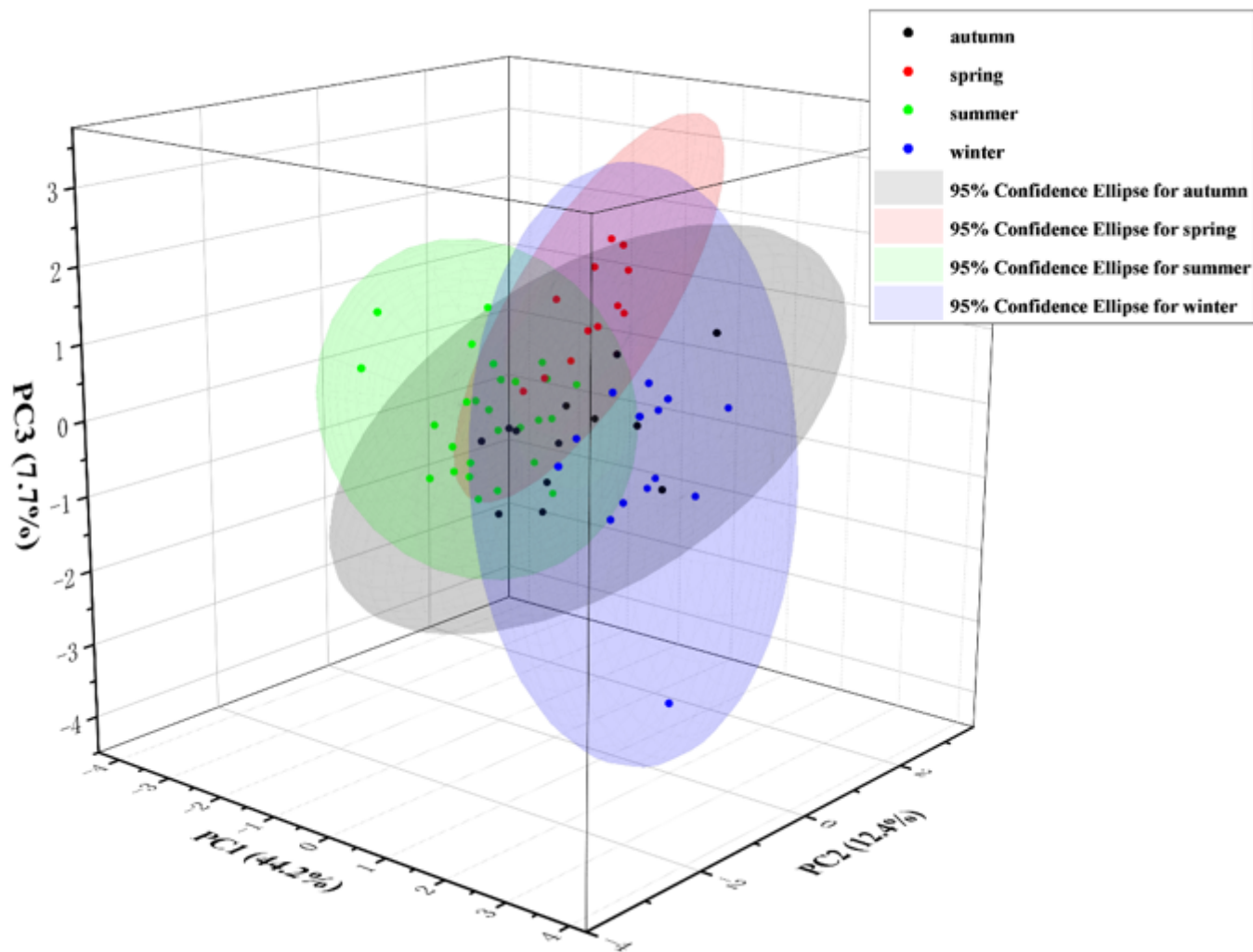


Figure 4

Principal component analysis (PCA) plot of PAH composition

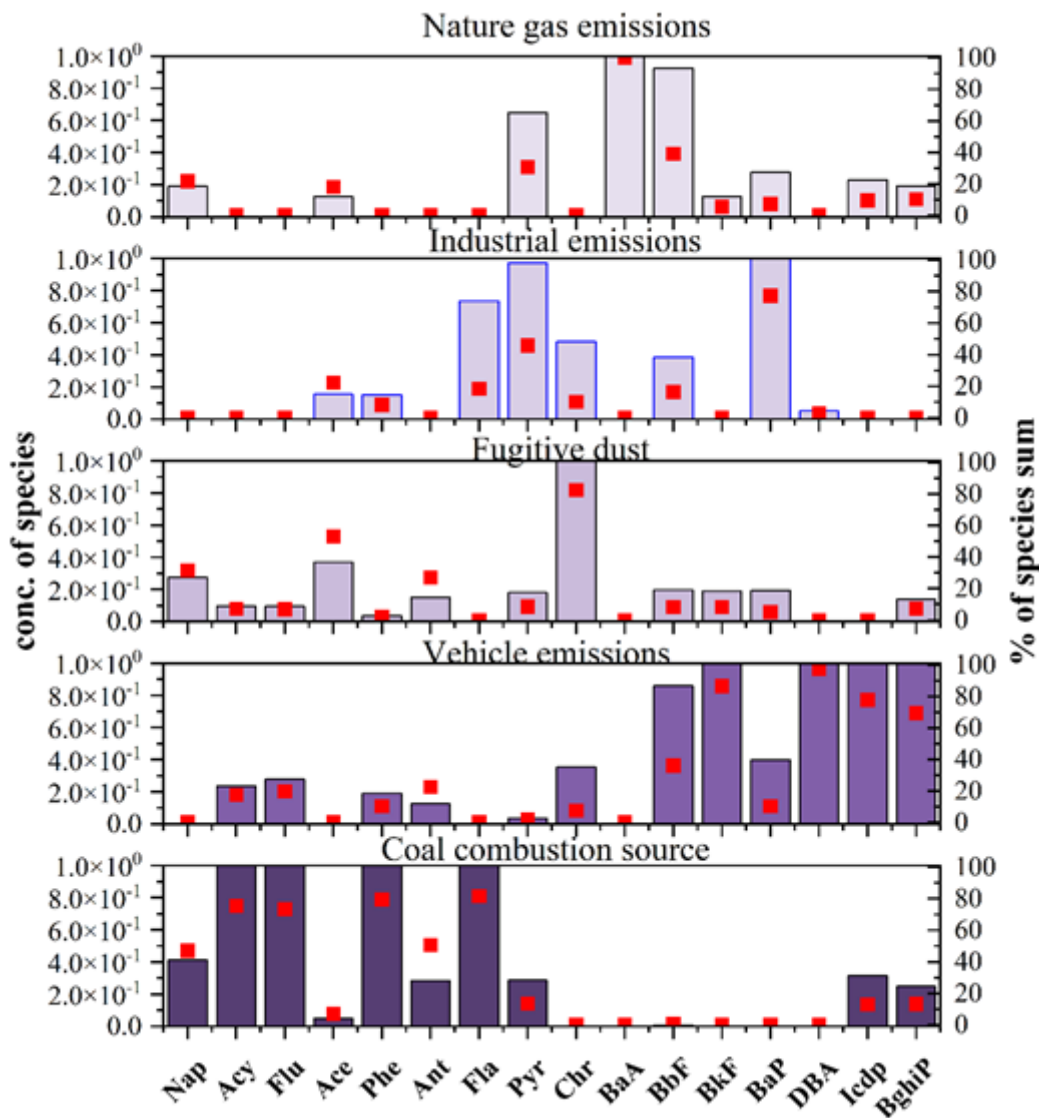


Figure 5

Sources profiles of PAHs identified from the PMF model for annual PAHs

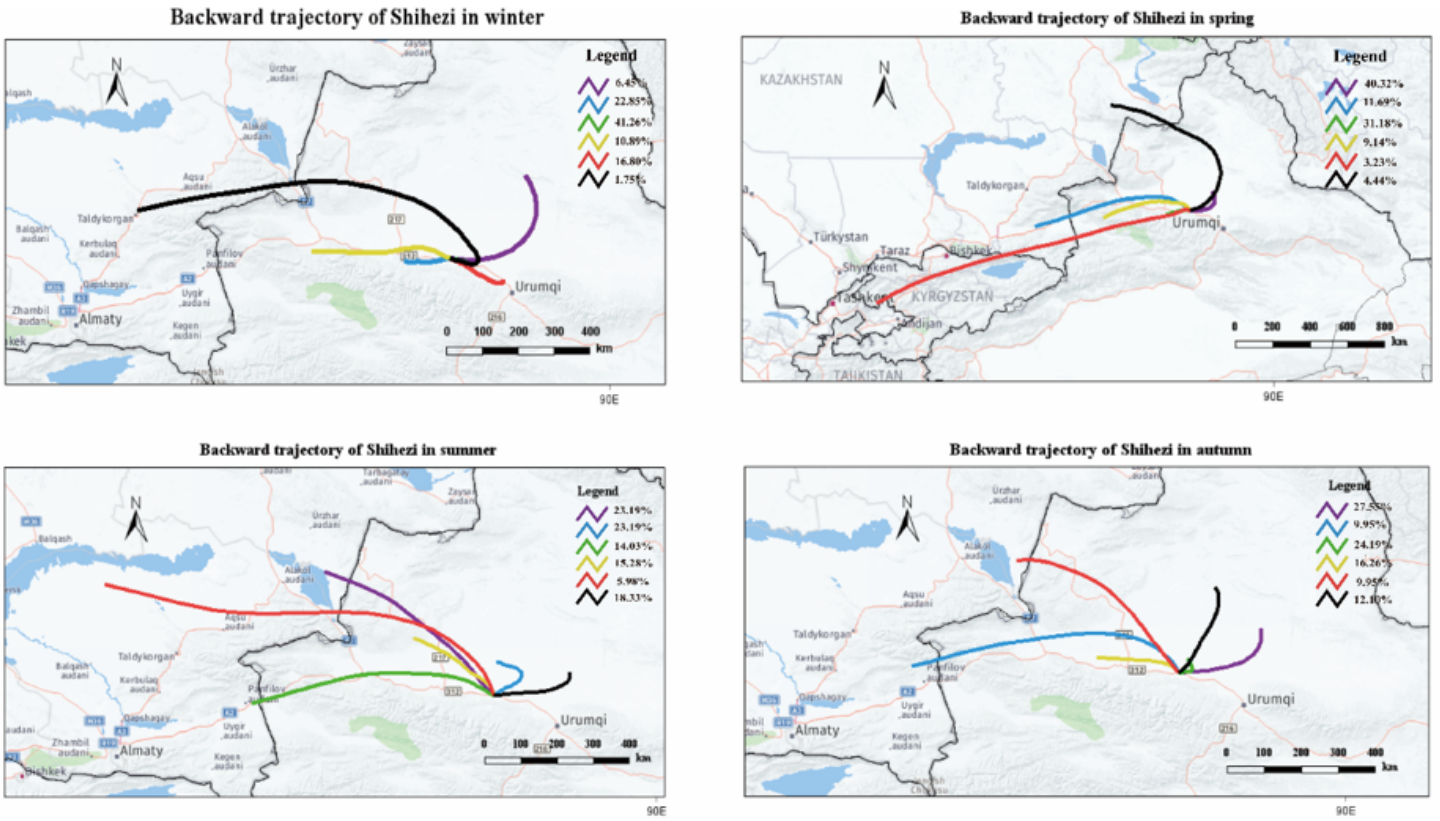


Figure 6

The backward trajectories cluster of PM_{2.5}-bound PAHs in Shihezi during each season.

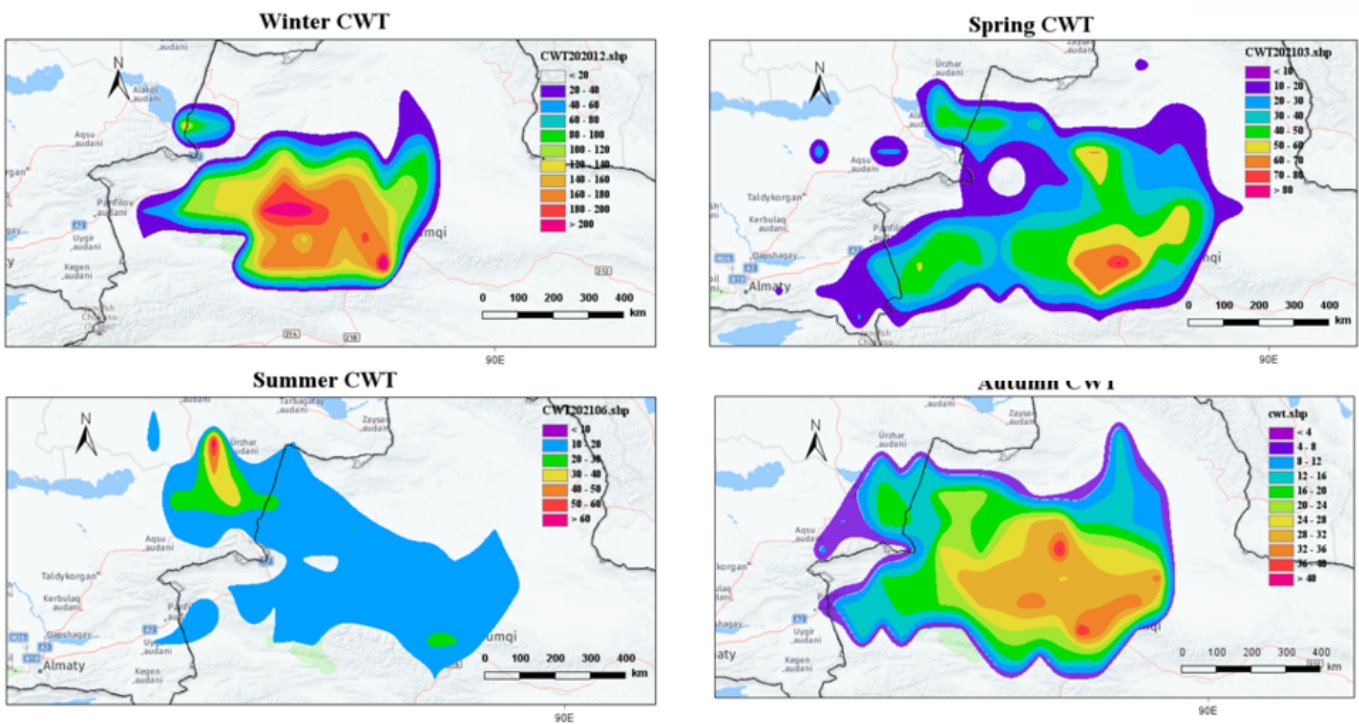


Figure 7

Potential sources of PM_{2.5}-bound form the CWT model.

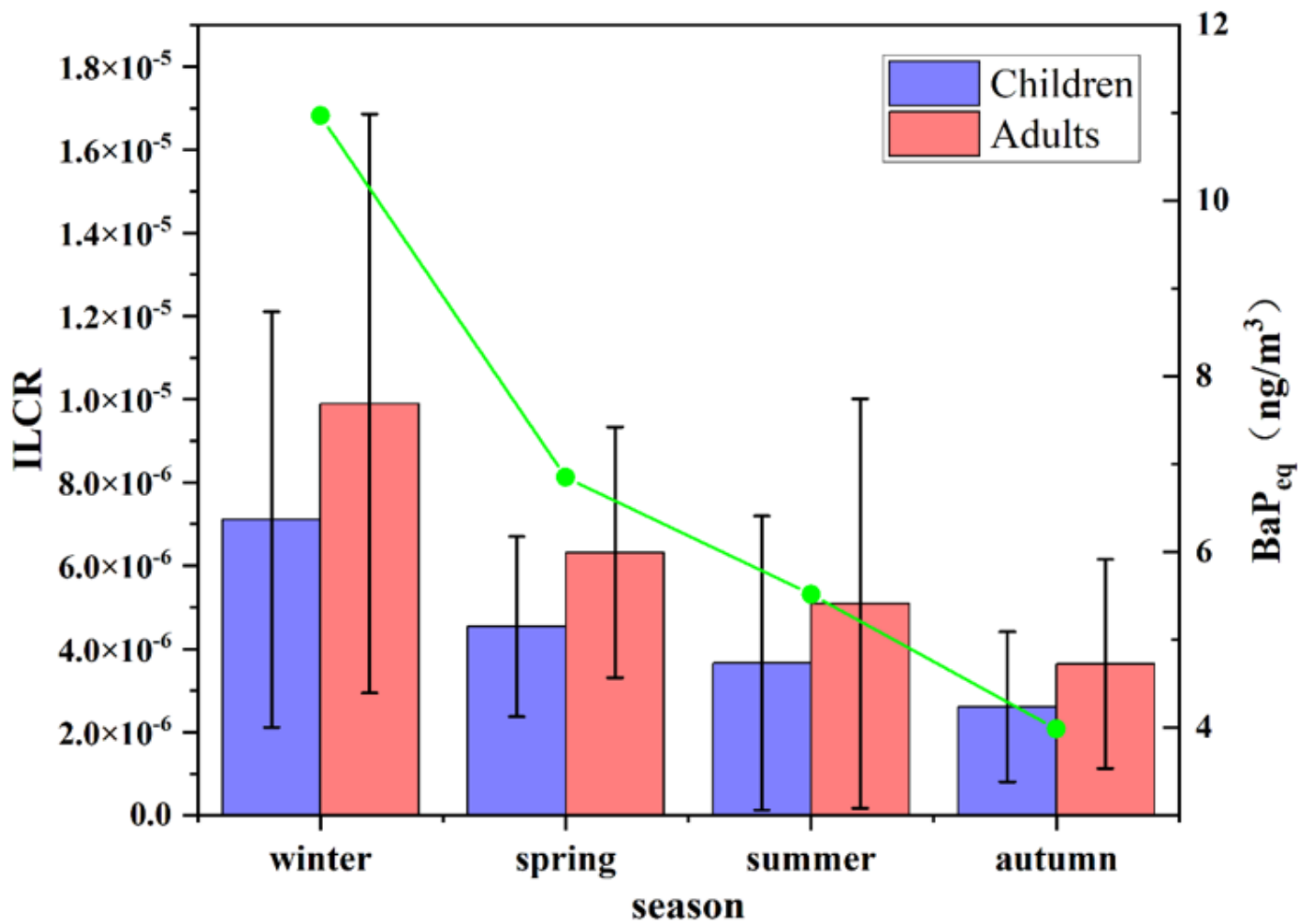


Figure 8

BaP_{eq} concentration and ILCRs from PAH inhalation exposure in four seasons.

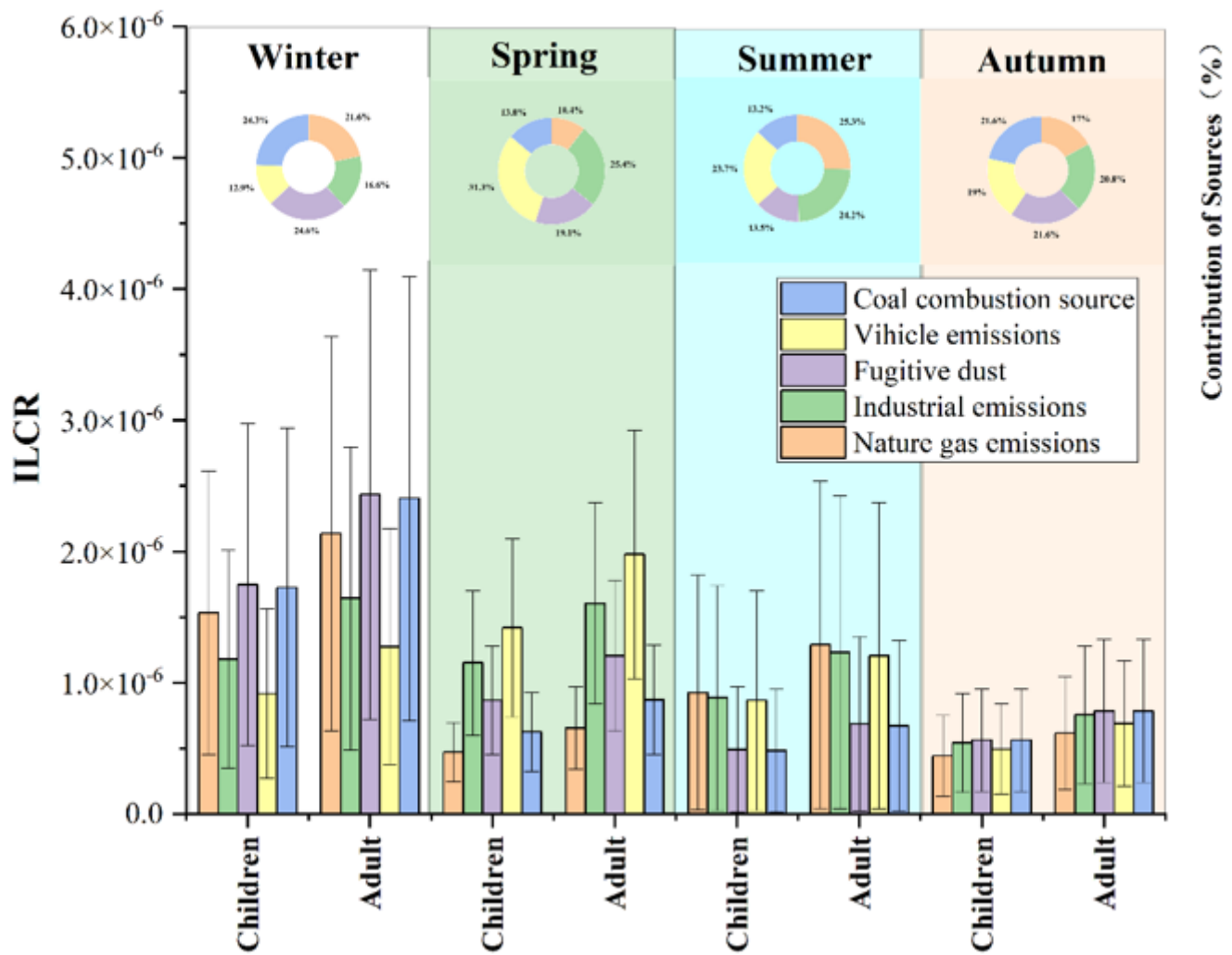


Figure 9

The ILCR and potential contributions of different emission sources in the four seasons.

Supplementary Files

This is a list of supplementary files associated with this preprint. Click to download.

- [Supplementaryinformation.docx](#)